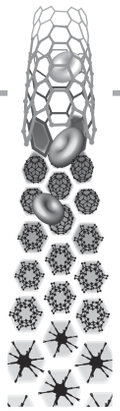

D-amino acid oxidase–nanoparticle system: a potential novel approach for cancer enzymatic therapy

Aim: The authors propose a new magnetic nanoparticle–enzyme system for cancer therapy capable of targeting the enzyme and consequently decreasing the adverse effects, meanwhile improving the patient's life quality. **Materials & methods:** The authors have functionalized Fe_3O_4 nanoparticles with 3-aminopropyltriethoxysilane (APTES) and conjugated it to yeast D-amino acid oxidase (DAAO) by coupling this with glutaraldehyde. **Results & conclusion:** The authors have tested the Fe_3O_4-APTES–DAAO system on three tumor cell lines. Exposed cells show, at the electron microscope level, nanoparticles on the surface of the plasma membrane and inside endocytic vesicles. Fe_3O_4-APTES–DAAO caused a substantial decrease of cell viability greatly augmented when D-alanine, a DAAO substrate, was added. Fe_3O_4-APTES–DAAO was demonstrated to be more effective than free DAAO, confirming the validity of the system in cancer therapy.

Original submitted 27 March 2012; Revised submitted 20 September 2012; Published online 5 February 2013

KEYWORDS: cell type ▪ cytotoxicity assay ▪ nanoparticle ▪ reactive oxygen species ▪ toxicity ▪ transmission electron microscopy

Adriana Bava[1], Rosalba Gornati*[1,2], Francesca Cappellini[1], Laura Caldinelli[1,2], Loredano Pollegioni[1,2] & Giovanni Bernardini[1,2]

[1]Dipartimento di Biotecnologie & Scienze della Vita, Università degli Studi dell'Insubria, Via Dunant 3, Varese, Italy

[2]'The Protein Factory' Research Center, Politecnico di Milano, ICRM-CNR Milano & Università dell'Insubria, Via Mancinelli 7, Milano, Italy

**Author for correspondence:*
Tel.: +39 033 242 1314
Fax: +39 033 242 1500
rosalba.gornati@uninsubria.it

Nano-oncology, the application of nanobiotechnology to the management of cancer, is currently a promising issue in nanomedicine. Nanoparticles (NPs) enable the targeted delivery of drugs to cancer cells [1–3]. This localized therapy improves efficacy and, at the same time, decreases adverse effects by reducing the dosage of anticancer drugs resulting in ameliorating the patient's quality of life [3]. Moreover, NPs are often capable of crossing various biological barriers [4–6] such as the blood–brain barrier, which limits the access to brain tumors. NPs can also penetrate solid tumors, where the access of drugs to malignant cells is often limited by the abnormal organization, structure and function of the blood vessels that form a barrier [7–11]. Several drugs, some of these already approved for human treatment, are based on nanobiotechnology and comprise different formulations of active principles. Liposomes (DaunoXome® [Gilead Sciences, CA, USA; daunorubicin], Doxil® [Janssen Biotech, Inc., PA, USA]/Caelyx® [Janssen, NSW, Australia] [doxorubicin]), polymer–protein conjugates (Oncaspar® [Enzon Pharmaceuticals, Inc., NJ, USA; PEG–L-asparaginase], SMANCS [Astellas Pharma, Inc., Tokyo, Japan; zinostatin]) and radioimmunoconjugates (Bexxar® [GlaxoSmithKline, Brentford, UK; anti-CD20 conjugated to iodine-131], Zevalin® [Spectrum Pharmaceuticals, NV, USA; anti-CD20 conjugated to yttrium-909]) are some examples of approved anticancer nanodrugs [1,12].

Among the innumerable approaches that can be used in the treatment of cancer, one of the oldest is based on the oxidative stress caused by reactive oxygen species. Radiation generates oxygen-derived free radicals and excited states; therefore, radiotherapy is one of the most common treatments of cancers [13]. On the other hand, radiotherapy poses the risk of secondary malignancy in the radiated area and its efficacy is often hindered by the emergence of radiation-resistant populations [14]. From the late 1950s to the early 1970s, injections of H_2O_2 into the tumor were performed, but this approach showed little therapeutic success [15]. Later, H_2O_2-generating enzymes, such as glucose oxidase or xanthine oxidase, were delivered in experimental tumors [16]. Unfortunately, the stability of the enzymes was low *in vivo* and, furthermore, their substrates (glucose, xanthine and oxygen) were endogenous molecules whose concentration could not be adequately modulated [17]. Therefore, there was a rationale for the use of other oxidizing enzymes whose activity could be regulated. D-amino acid oxidase (DAAO; EC 1.4.3.3) represents a good choice: its favorite substrate, D-Ala, can be found endogenously in very small amounts; therefore, H_2O_2 production can be modulated by the delivery of an appropriate dose of D-amino acids. Owing to its availability as a recombinant protein and peculiar biochemical characteristics, such as high specific activity, tight binding with

Future Medicine part of fsg

the flavin adenine dinucleotide cofactor and good thermal stability [18], *Rhodotorula gracilis* DAAO (RgDAAO) was proposed as a suitable candidate to produce reactive oxygen species in tumors [19]. A main drawback in the use of native RgDAAO is the comparatively high K_m for oxygen (~2 mM) [20] versus the local oxygen concentration (estimated at ~25 µM in growing tumors). A RgDAAO variant possessing a tenfold lower $K_{m,O2}$ was produced by a directed evolution approach. This evolved enzyme, containing five point mutations, induced remarkably increased cytotoxicity effects on mouse tumor cells [21].

In this context, a possibility to improve the efficacy of cancer therapy would also be to combine the advantages of using NPs, especially magnetic NPs such as magnetite and maghemite, with those of an enzyme with a well-known and controlled anticancer effect, such as DAAO. The authors have chosen magnetic NPs as they offer some attractive possibilities in biomedicine for a variety of important reasons. First, they have controllable sizes in the range of those of a virus, which can be exploited to reach poorly accessible districts. Second, they can be manipulated by a magnetic field. This property, combined with the intrinsic penetrability of magnetic fields into human tissue, makes them particularly interesting in guiding an anticancer drug directly to a tumor. Third, magnetic NPs can be heated by a magnetic field to trigger drug release or to produce hyperthermia and tissue ablation [22–24]. Fourth, magnetic NPs can be efficiently visualized by MRI giving the same system both therapeutic and diagnostic (theranostic) functions [25].

To optimize this oxystress-based cancer therapy, Fe_3O_4 NPs were functionalized with 3-aminopropyltriethoxysilane (APTES) and conjugated to RgDAAO to produce Fe_3O_4-APTES–DAAO. This system has been studied by *in vitro* tests of cytotoxicity and uptake to check for its capability to kill human cancer cells. To this aim, three different tumor cell lines (human ovary adenocarcinoma SKOV-3, human glioblastoma U87 and human colorectal carcinoma HCT116) have been used. This investigation could help to develop a new, more effective treatment especially for brain tumors, which are isolated by the blood–brain barrier, and for solid tumors where the access of drugs is often limited by poor vascularization and areas of necrosis [7]. In particular, brain tumors are intrinsically more complicated to treat than systemic malignancies; this depends on the type, location and size of the tumor, the patient's age and general health, as well as the blood–brain barrier-induced diffusion limitation, which impedes chemotherapeutic agents from reaching brain neoplasms. For all of these reasons, brain tumors are treated with surgery, radiation therapy and chemotherapy with a low recovery rate [26]. In this context, an alternative system for cancer therapy is desiderable and nanosystems can bring significant innovations over conventional formulations with respect to decreased toxicity and improved pharmacokinetic and pharmacodynamic properties [27–29].

Materials & methods

Chemicals

Iron oxide NPs, Fe_3O_4 NPs (nanopowder: <50 nm particle size), APTES (purity: >98%) and all other reagents (cell culture grade) were purchased from Sigma-Aldrich (Milan, Italy). Horseradish peroxidase was purchased from Roche (Milano, Italy), CellTiter-Glo® Luminescent Cell Viability Assay was purchased from Promega (WI, USA). RgDAAO variants were produced as recombinant proteins in *Escherichia coli* and purified as stated in [30]. The final enzyme preparation equilibrated in 50 mM potassium phosphate buffer at pH 7.5, 2 mM EDTA, 10% v/v glycerol and 5 mM 2-mercaptoethanol, had a specific activity of approximately 90 U/mg protein at 25°C, 21% oxygen and on D-Ala as a substrate. Milli-Q Ultrapure Water System (Millipore, MA, USA) was used.

Coating of magnetic NPs

Fe_3O_4-APTES

A 5-ml APTES solution (2% w/v final concentration) was added to a well-dispersed suspension of 150 mg of Fe_3O_4 NPs in 10 ml water, and maintained under mechanical stirring at 50°C for 5 h according to del Campo *et al.* [31]. The Fe_3O_4-APTES were separated from unbound APTES by a commercial parallelepiped neodymium magnet (Webcraft GmbH, Uster, Switzerland; Ni–Cu–Ni plated; magnetization: N45; size: 30 × 30 × 15 mm), washed several times with water, anhydrificated with ethanol and dried overnight at 50°C.

Fe_3O_4-APTES–DAAO

A suspension of 4 mg of Fe_3O_4-APTES in 2 ml glutaraldehyde (0.5% v/v) obtained by ultrasonication for 1 min (Sonica® 5300MH; Soltec, Milano, Italy) was allowed to react for 2 h using a rotating plate tube stirrer at room temperature. The produced adduct was separated from the supernatant with a neodymium magnet, washed three times with 500 µl of distilled water,

then with 500 µl 5 mM sodium pyrophosphate buffer (NaPPi) at pH 8.5. Functionalized Fe_3O_4 NPs were resuspended in 5 mM NaPPi at pH 8.5 and the mixture sonicated for 1 min. Finally, 250 µg of pure RgDAAO was added (1 ml of final volume) and the reaction was carried out for 4 h at 4°C using a rotating plate tube stirrer. Subsequently, Fe_3O_4-APTES–DAAO were collected by a magnet and washed twice with 500 µl of 5 mM NaPPi. The supernatant was stored for further analysis.

The same procedure has been used to prepare the system Fe_3O_4-APTES–DAAO(R285A), in which the Arg (R) 285 in the active site has been substituted with an Ala (A) generating a nonactive RgDAAO mutant [32].

Spectra analysis

The amount of protein bound to Fe_3O_4 NPs was determined as the difference between the starting amount of RgDAAO and the protein recovered in the supernatant at the end of reaction. Quantification was performed using the extinction coefficient at 455 nm (~12.6 $mM^{-1}cm^{-1}$) using an UV-Vis V-560 Spectrophotometer (JASCO, MD, USA).

Characterization of the NP-coated samples was performed using the solid phase Fourier transform infrared spectroscopy: spectra were collected on a Nicolet Avatar 360 Spectrometer (JASCO). Samples were mixed with infrared grade KBr in a proportion of 2:100 (w/w).

RgDAAO activity assay

The activity of Fe_3O_4-APTES–DAAO and Fe_3O_4-APTES–DAAO(R285A) was determined by measuring the absorbance increase accompanying the H_2O_2-induced oxidation of *o*-dianisidine. One DAAO unit corresponds to the amount of enzyme that converts 1 µmol of substrate per min at 25°C and at 0.253 mM oxygen concentration [33]. The standard assay mixture contained 890 µl of 100 mM D-Ala in 100 mM NaPPi buffer, pH 8.5, 100 µl 3.2 mg/ml *o*-dianisidine in water, 10 µl of 0.4 mg/ml horseradish peroxidase in 100 mM NaPPi buffer, pH 8.5, and 10 µl of 0.4 mg/ml Fe_3O_4-APTES–DAAO in the same buffer. The reaction was initiated by the addition of the enzyme and the absorbance increase was monitored at 440 nm for 1 min using an UV-Vis V-560 Spectrophotometer. The initial velocity at different substrate concentrations (0.1–100 mM) were recorded and used to calculate the apparent kinetic parameters using the KaleidaGraph 4.0 software (Synergy Software, PA, USA).

HPLC measurements

D- and L-serine cellular concentrations were determined according to Sacchi *et al.* [34]. In detail, a fixed amount (5×10^5 cells) of SKOV-3 or U87 cells were homogenized in 1 ml of 5% cold trichloroacetic acid and then centrifuged at 16,000 × *g* for 45 min at 4°C. Trichloroacetic acid was stripped six times from the supernatant using diethylether before lyophilization and storage at -20°C. Lyophilized cell samples were dissolved in 90 µl of 0.1 M sodium borate buffer, pH 10.4. For amino acid derivatization, 3 µl of U87 or 15 µl of SKOV-3 samples were treated with 24 µg of *N*-acetyl-cysteine and 7.5 µg of *o*-phthaldialdehyde in 0.1 M sodium borate buffer, pH 10.4.

HPLC separations were performed on a Symmetry® Column C8 (Waters, Milano, Italy; 5 µm) kept at 30°C using a JASCO HPLC system. Flow rate was set at 1 ml/min; L- and D-serine were eluted with an isocratic method using 0.1 M sodium acetate and 1% tetrahydrofuran at pH 6.2. Derivatized amino acids were detected using a fluorescence detector: excitation at 344 nm and emission at 443 nm. D- and L-serine quantification was performed by a calibration curve set up using increasing concentrations of standard D-serine (0.25–10 pmol) and L-serine (10–200 pmol).

Cell culture test

SKOV-3 and HCT116 cell lines were maintained as adherent cells in RPMI1640 medium, while U87 cell lines were maintained in DMEM medium, at 37°C in a humidified 5% CO_2 atmosphere. RPMI1640 medium was supplemented with 10% fetal bovine serum, 1% L-glutamine and 1% penicillin/streptomycin solution, whereas DMEM medium was supplemented with 10% fetal bovine serum, 1% L-glutamine, 1% penicillin/streptomycin and 1% sodium pyruvate. Cells were passaged as needed using 0.25% trypsin–EDTA.

Cell viability

Cell viability was determined as ATP content by using the CellTiter-Glo Luminescent Cell Viability Assay according to the manufacturer's instruction. In detail, 200 µl of cell suspension (containing 2×10^4, 1×10^4, 5×10^3 or 25×10^2 cells, depending of the exposure time) were seeded into 96-well assay plates and cultivated for 24 h at 37°C in 5% CO_2 to equilibrate and become attached prior the treatment. Cells were then exposed to increasing amounts of naked Fe_3O_4 NPs for 0.5, 1, 2, 24, 48 and 72 h. In

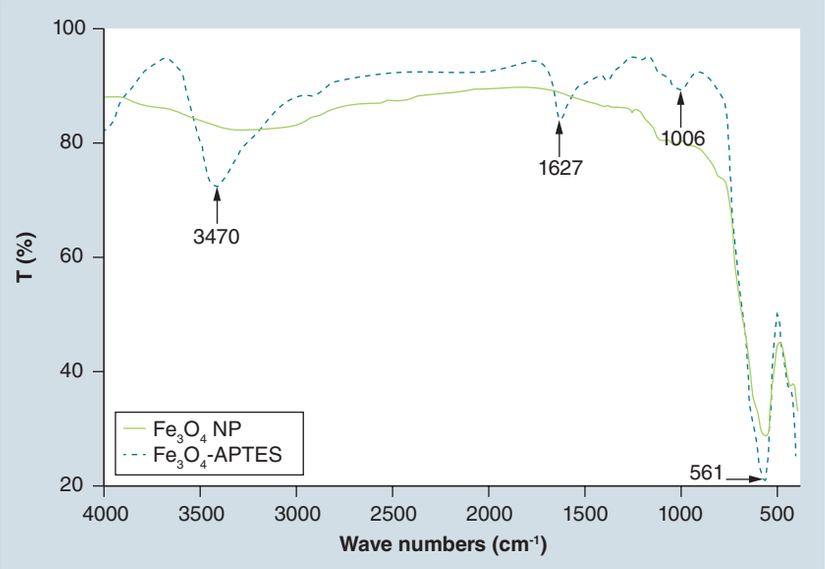

Figure 1. Fourier transform infrared spectra. The peak at 561 cm^{-1} indicates the Fe-O bond; the peak at 1006 cm^{-1} indicates the Si-O bond and the peak at 1627 cm^{-1} is assigned to the bending N-H bond. The peak at 3470 cm^{-1} corresponds to the N-H stretching vibrations of the -NH_2 group overlapped to hydrogen-bonded silanols.
Fe_3O_4-APTES: Fe_3O_4 nanoparticles functionalized with 3-aminopropyltriethoxysilane; NP: Nanoparticle.

another series of experiments, 1×10^4 cells were exposed to increasing amounts of free DAAO or Fe_3O_4-APTES–DAAO for 24 h. Following the treatment, plates were equilibrated for 30 min at room temperature and 100 µl of CellTiter-Glo Reagent was then added to each well. Plates were shaken for 2 min and left at room temperature for 10 min prior to the recording of luminescent signals using the Infinite F200 plate reader (Tecan Group, Männedorf, Switzerland). For all cell lines, experiments were performed in triplicate. Cell viability, expressed as ATP content, was normalized against control values. The same procedure has been used for free DAAO (R285A) and Fe_3O_4-APTES–DAAO (R285A).

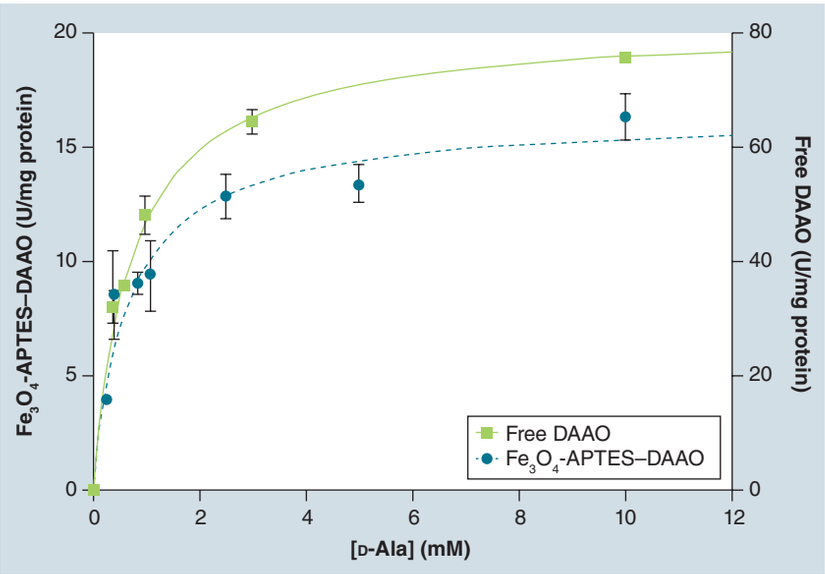

Figure 2. Michaelis–Menten plot of the activity measured for Fe_3O_4-3-aminopropyltriethoxysilane-D-amino acid oxidase and free D-amino acid oxidase at increasing D-Ala concentrations.
DAAO: D-amino acid oxidase; Fe_3O_4-APTES: Fe_3O_4 nanoparticles functionalized with 3-aminopropyltriethoxysilane.

Cellular uptake

Cellular uptake and localization was determined on SKOV-3, U87 and HCT116 cells exposed to Fe_3O_4-APTES–DAAO for 24 h and analyzed by transmission electron microscopy. For transmission electron microscopy studies, exposed cells were harvested, fixed in 2% glutaraldehyde in 0.1 M sodium cacodylate buffer (pH 7.2) for 10 min on ice and for 30 min at room temperature, washed in the same buffer, and postfixed in dark for 1 h with 1% osmiun tetroxide in 0.1 M sodium cacodylate buffer (pH 7.2) at room temperature. After standard steps of serial ethanol dehydration, samples were embedded in an Epon-Araldite 812 1:1 mixture (Sigma-Aldrich). Thin sections (80 nm) were obtained with a ReichertUltracut S ultratome (Leica, Wetzlar, Germany), stained by standard methods with uranyl acetate and lead citrate, and observed with a JEOL 1010 electron microscope (JEOL, Tokyo, Japan) operated at 90 kV.

Statistics

Kinetic data and cell viability values were expressed as mean ± standard deviation. Statistical tests were performed using KaleidaGraph 4.0 software (Synergy Software).

Results

Sample characterization

Fe_3O_4-APTES were produced by a simple and fast procedure described in the 'Materials & Methods' section. Figure 1 reports Fourier transform infrared spectra of Fe_3O_4 NPs and Fe_3O_4-APTES. The peak within 550–570 cm^{-1} is characteristic of Fe-O vibrations related to the magnetite core. The presence of silane on the surface of NPs (Figure 1) is confirmed by the presence of characteristic peaks; the peak at 1006 cm^{-1} is indicative of the Si-O bond; the peaks at 3470 and 1627 cm^{-1} are indicative of the N-H stretching and bending vibrations overlapped with those of vibration bands of hydrogen-bonded silanols (SiOH groups). Fe_3O_4-APTES expose the -NH_2 groups, allowing NPs to remain dispersed in the medium.

Assessment of binding efficiency

RgDAAO was conjugated to Fe_3O_4-APTES by means of glutaraldehyde. Under the authors' best experimental conditions, the amount of enzyme bound to NPs, determined as the difference between the protein amount added and that recovered in the supernatant, is approximately 70%, with an enzymatic activity of approximately 4.5 U/mg NP. DAAO activity remained stable for 2 weeks at 4°C and a 20% decrease was observed after 2 months. The coating procedure did not affect the kinetic properties of RgDAAO. In fact, the apparent K_m of the immobilized enzyme for D-Ala was identical to that of the free enzyme (0.9 vs 1 mM) (Figure 2) [18]. Altogether, this conjugation procedure does not seem to alter the flavoenzyme conformation and its binding with the flavin adenine dinucleotide cofactor, which is absolutely required for its catalytic activity.

Cytotoxicity studies

Cytotoxicity was tested on three different tumor cell lines, that is, SKOV-3 (ovarian adenocarcinoma), HCT116 (colorectal carcinoma) and U87 (glioblastoma and astrocytoma). The effects of the different forms of DAAO on cell viability, expressed as ATP content, are reported in Figure 3. In absence of the D-Ala addition, free DAAO, at the tested doses, did not affect viability of the three tested cell lines. To induce the cytotoxic stress, D-Ala was used since it represents the reference substrate for DAAO [18]. Noteworthily, D-Ala itself had no effect on cell viability at the used concentrations [Bava, Gornati, Cappellini *et al.*, Unpublished Data]. When D-Ala was added, a clear effect was seen in SKOV-3 (Figure 3A) and HCT116 (Figure 3B) cell lines, while U87 glioblastoma cells were insensitive to the treatment (Figure 3C).

Fe_3O_4-APTES–DAAO, with and without its substrate, was also tested. As far as it concerns cytotoxic effects, the effect of Fe_3O_4 NPs at the concentrations used in these experiments is negligable (Supplementary Data; see online at www.futurescience.com/doi/suppl/10.2217/NNM.12.187). As shown in Figure 3, Fe_3O_4-APTES–DAAO also exert a certain degree of toxicity in the absence of the substrate addition. In all cases, however, the cytotoxicity is increased by D-Ala addition. It is noteworthy that Fe_3O_4-APTES–DAAO in the presence of 1 mM D-Ala completely depletes the ATP content already at 3.5 mU of the enzyme.

U87 glioblastoma cells were generally less

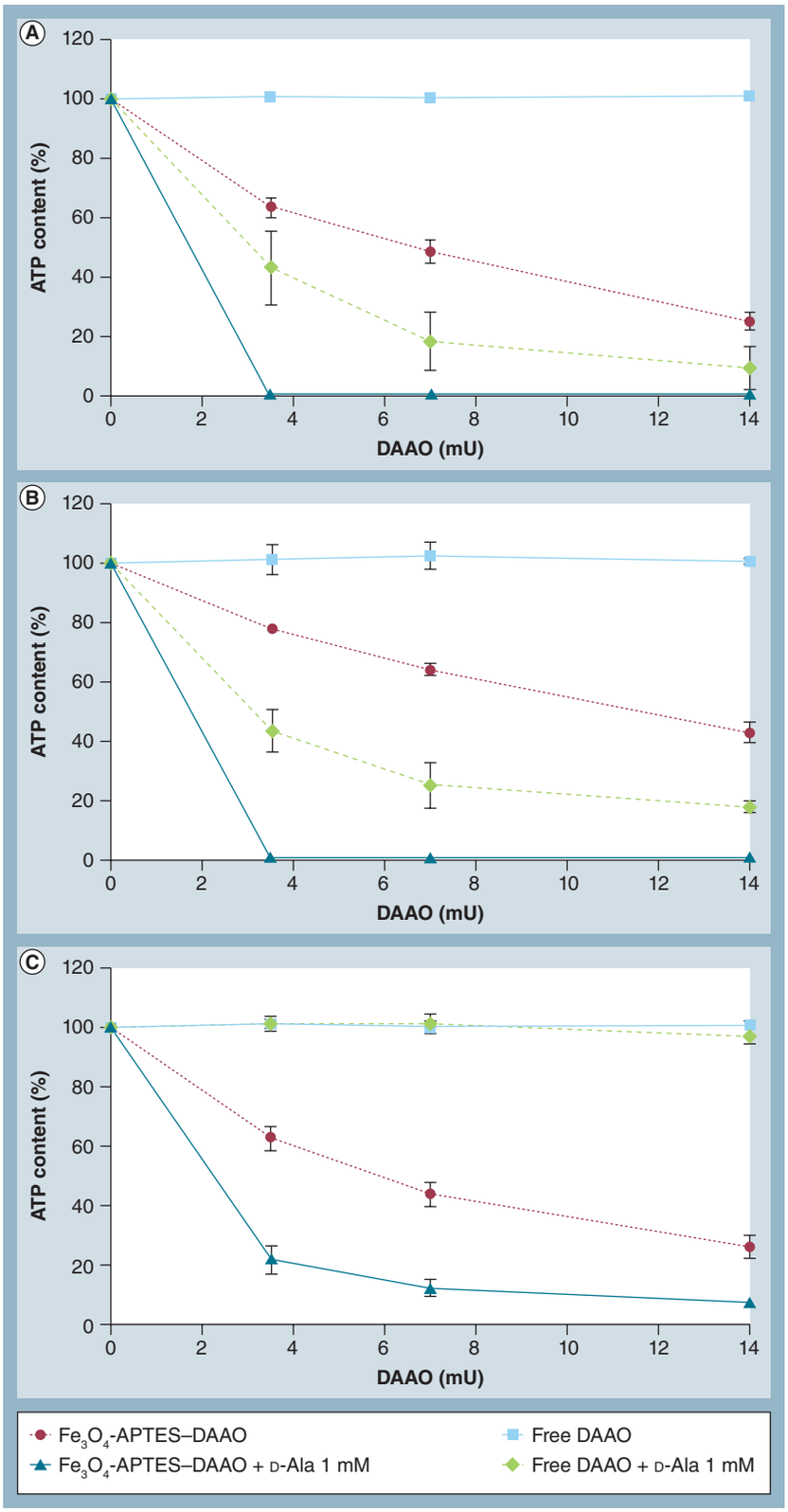

Figure 3. Cell viability. (A) SKOV-3; **(B)** HCT116; and **(C)** U87 cell lines. Cell viability is expressed as a percentage of ATP content compared with control after a 24-h exposure to 3.5, 7 and 14 mU of Fe_3O_4-APTES–DAAO and free DAAO, with and without the substrate D-Ala.
DAAO: D-amino acid oxidase; Fe_3O_4-APTES-DAAO: Fe_3O_4 nanoparticles functionalized with 3-aminopropyltriethoxysilane and bound to D-amino acid oxidase.

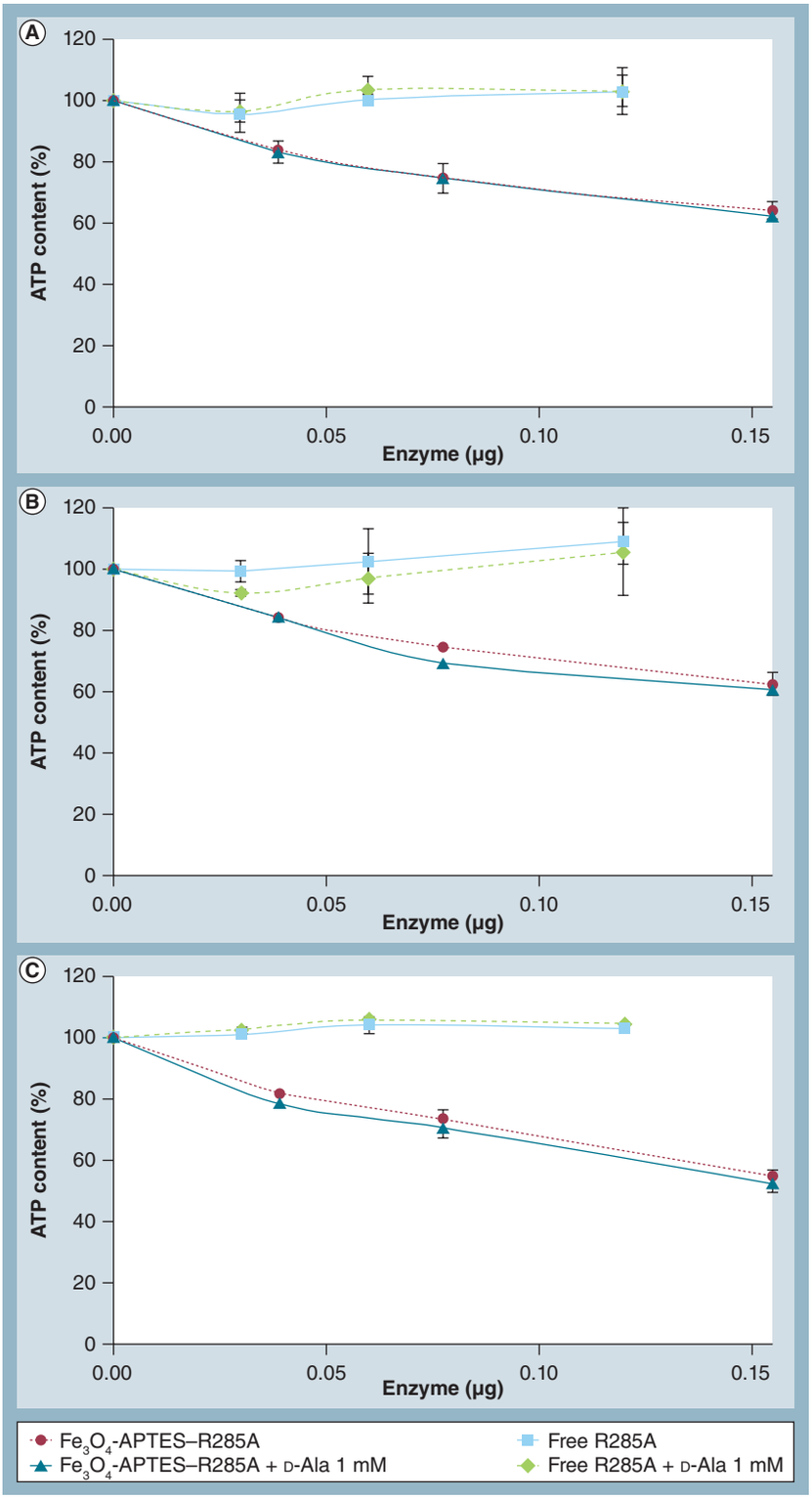

Figure 4. Cell viability expressed as percentage of ATP content compared with control. (A) SKOV-3; **(B)** HCT116; and **(C)** U87 cell lines after a 24-h exposure to the nonactive D-amino acid oxidase mutant R285A, with and without the substrate D-Ala. The mutant was either free (0.03, 0.06 and 0.012 µg of enzyme) or bound to Fe_3O_4-APTES (0.04, 0.08 and 0.015 µg of enzyme).
Fe_3O_4-APTES–R285A: Fe_3O_4 nanoparticles functionalized with 3-aminopropyltriethoxysilane and bound to D-amino acid oxidase mutant R285A.

sensitive to the treatment (Figure 3C). To check for a possible presence of endogenous D-amino acids, D-Ser in U87 was measured and compared with its presence in SKOV-3. D-Ser is a well-known neuromodulator, which represents the most abundant natural D-amino acid in different brain cells [35]. HPLC analysis showed that the cellular D-Ser content was approximately 1% of the total (L- and D-) serine levels in both cell lines. Accordingly, if oxidized by DAAO, the natural content in D-Ser should result in the same H_2O_2 production and, thus, should similarly affect the viability of cell lines during treatment.

To confirm that the toxicity was mainly due to the enzyme activity, cells were also exposed, in the same conditions previously used, to DAAO(R285A), a nonactive mutant. The results, reported in Figure 4, confirmed that the free DAAO(R285A) in presence or not of 1 mM of D-Ala does not affect ATP content, while the system Fe_3O_4-APTES–DAAO(R285A), even at the highest dose, accounts, at most, for 40% of ATP reduction.

NP uptake

As already reported [36], NPs are able to enter the cells by endocytosis, probably by binding to the membrane (Figures 5 & 6). Cañete *et al.* have demonstrated that iron oxide NPs enter the cells mainly by a macropinocytosis process and not by a clathrin-mediated endocytosis [37]. NP uptake seems a requisite to exert their maximum toxicity. Internalization of the particles was rapid, aspecific and concentration dependent [Bava, Gornati, Cappellini *et al.*, Unpublished Data]. In Figures 5 & 6, where SKOV-3 and U87 cells exposed to Fe_3O_4-APTES–DAAO for 24 h are reported as examples, cellular pseudopodes, characteristic structures of the endocytosis pathway, are particularly evident. Once entered into the cell, the majority of NPs remain in the cytoplasm inside the endocytic vesicles. Nevertheless, vesicles may undergo mechanical damage, freeing NPs, which could reach different cell districts such as mitochondria where they are seen by transmission electron microscopy (Figure 5B).

Discussion

The authors have focused their research on the synthesis and characterization of magnetic NPs combined with the enzyme DAAO as a potential drug for cancer treatment. They took advantage of the use of a very active flavoenzyme capable of producing H_2O_2 by oxidation of a specific substrate, such as a D-amino acid. These compounds are scarcely present in human

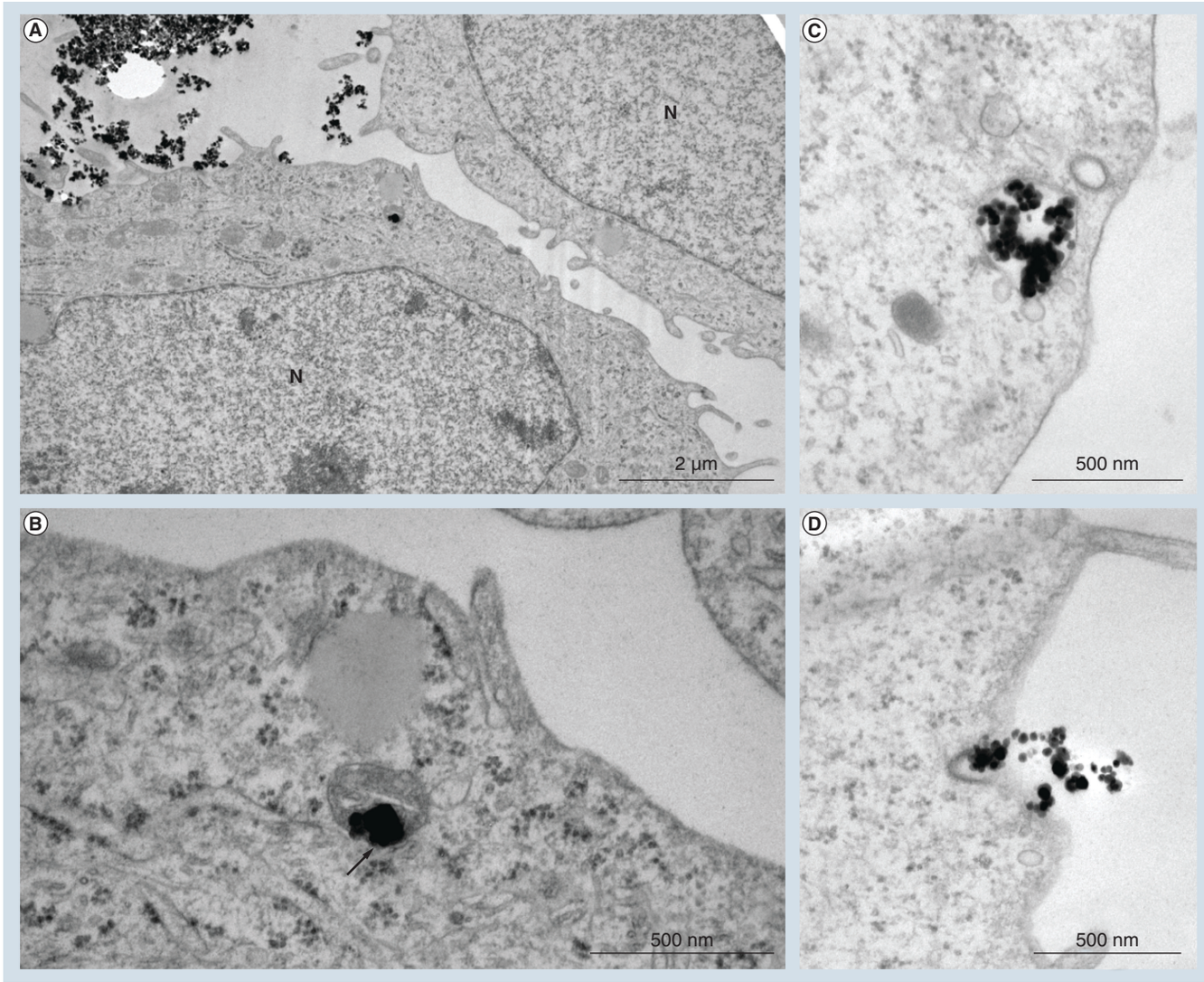

Figure 5. Transmission electron microscopy pictures of SKOV-3 cells exposed to Fe_3O_4 nanoparticles functionalized with 3-aminopropyltriethoxysilane for 24 h. (A) Several electron opaque particles in the extracellular space and adhering to the plasma membrane. Particles are also visible inside the cell. **(B)** The enlargement of **(A)** shows particles in correspondence of a mitochondrion (arrow). Particles are also visible **(C)** inside a vesicle and **(D)** on the surface of the cell suggesting membrane invagination.
N: Nucleus.

tissues, so it is possible to control the production of H_2O_2 by adjusting the concentration of the substrate to be administered [19,21]. For a recent, general review on the use of oxidative stress for cancer therapy, see [7,38,39].

In this work, RgDAAO covalently linked to Fe_3O_4 NPs by free -NH_2 groups of APTES activated by glutaraldehyde was used. The presence of aminosilane has been confirmed by Fourier transform infrared spectroscopy analysis and, as reported in the literature [40,41], the peaks found at 1006, 1627 and 3470 cm^{-1} are characteristic of the Si-O bond and -NH groups present in the APTES molecule (Figure 1). Under the authors' best experimental conditions, they were able to immobilize approximately 70% of the free enzyme. The system (i.e., Fe_3O_4-APTES–DAAO) showed an activity of 4.5 U/mg of NP and an apparent K_m for the substrate D-Ala similar to that determined for the free enzyme. Unfortunately, the results are difficult to compare with the data present in literature [42,43] due to the disparate experimental conditions that were used. However, Hsieh *et al.* reported that they were able to immobilize approximately 80% of the free enzyme, but with a relatively low recovered activity [44]. A problem associated with the use of magnetic NPs is represented by the safe dose of accumulation to avoid side effects. The system allows for a minimal amount of Fe_3O_4 NPs (~6 µg) to be used, whose intrinsic cytotoxicity

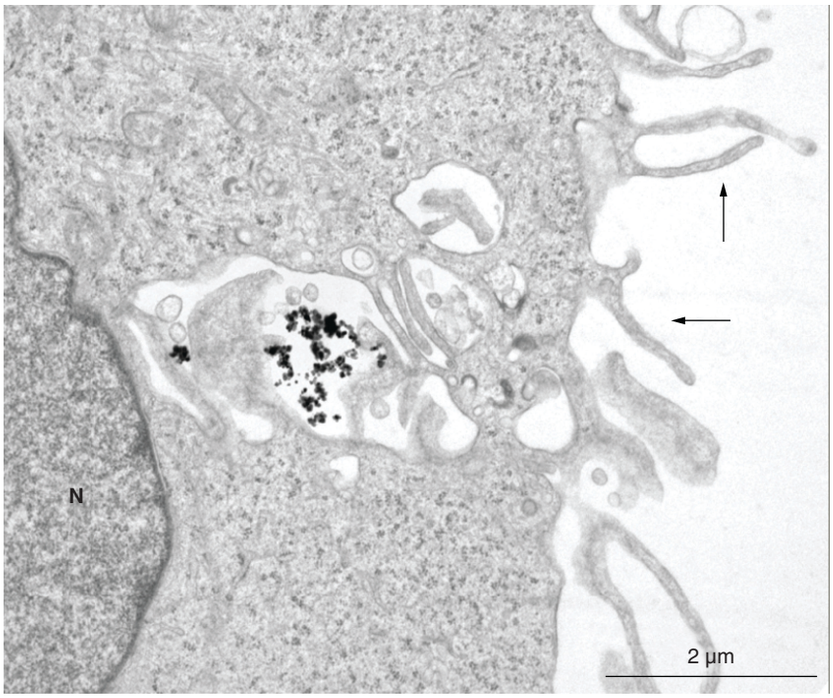

Figure 6. Transmission electron microscopy image of U87 cells exposed to Fe_3O_4 nanoparticles functionalized with 3-aminopropyltriethoxysilane for 24 h. Electron opaque particles are entrapped in intricate membrane morphology. Arrows indicate the pseudopodes.
N: Nucleus.

is approximately 20% for the examined cell lines (see Supplementary Data and [45–47]).

NP cellular uptake, studied in a wide variety of cell types, has revealed a conserved mechanism characterized by an inverse relationship between the internalization and NP size; furthermore, the uptake machinery depends on the cell-loading conditions, including surface charge, particle concentration and properties, and incubation time [48,49]. For high concentrations and long exposure times, such as those used in these experiments (system concentration of 80 µg/ml and exposure time of 24 h), the process was not dependent on the aforementioned parameters. This assertion has been confirmed by experiments showing a similar behavior of system Fe_3O_4-APTES–DAAO towards all of the tested cell lines, both in the presence and absence of 1 mM of D-Ala. One advantage of this formulation is its efficacy in killing cells when administered together with its substrate and the relatively less efficacy when the treatment does not include the D-Ala, independently of cell type used. D-amino acids are normally present in the tissues, although at a much lower concentration than that of the L-amino acids. Therefore, a minimal activity of the enzyme in the absence of the exogenous substrate is also expected. Such activity is augmented by the fact that the system Fe_3O_4-APTES–DAAO probably exerts its function close to the cell membranes or inside the cells (Trojan horse effect). However, the toxicity of the system is dramatically increased by substrate addition and the difference is particularly evident at lower doses. A second main advantage is the very low amount of enzyme required to give maximal toxicity; the system Fe_3O_4-APTES–DAAO appears more efficient compared with that proposed by Divakaran *et al.* [50]. They reported the antitumor activity of a NP-DAAO system, prepared by electrostatically binding pig kidney DAAO to polyvinylpyrrolidone-coated Fe_2O_3 NPs. RgDAAO, in fact, is tenfold more active than pig kidney DAAO and the D-Ala concentration used in these experiments is dramatically lower. Moreover, the covalent link of RgDAAO to the NPs should confer a greater stability to the system.

After the exposure of cells with Fe_3O_4-APTES–DAAO, the NP system is probably confined in endosomal vesicles for a long time without affecting cell phenotype and function, even though long-term biotransformation is supposed to occur [48].

The effect of free RgDAAO whose behavior depends on the cell type is different. In fact, as shown in Figures 3A & 3B, significant toxicity is observed with free RgDAAO in the presence of 1 mM of D-Ala on SKOV-3 and HCT116 cell lines, while U87 glyoblastoma cells were totally insensitive (Figure 3C).

This behavior can be explained considering that free RgDAAO exerts its action in the extracellular environment, whose characteristics (pH, redox capability and presence of metabolites) can change depending on the cell type. Moreover, cell lines respond differently to reactive oxygen species insults. In any case, the fact that the effect of this nanosystem was due to the enzyme was confirmed by the relative ineffectiveness of the system Fe_3O_4-APTES–DAAO(R285A) (Figure 4).

Conclusion

Our experiments demonstrated that Fe_3O_4-APTES–DAAO was more effective than free RgDAAO, and independent of cell type, in inducing cytotoxicity, thus supporting the validity of the combination of Fe_3O_4-APTES–DAAO/D-Ala as a possible treatment in cancer therapy.

Future perspective

The potentiality of this system should be verified by studying tissue distribution, toxicity and

clearance after intravenous injection. DAAO is an enzyme that catalyzes the stereoselective deamination of D-amino acids generating H_2O_2 and, therefore, it may be regarded as a promising anticancer therapeutic. Its combination with magnetic NPs will allow the area of interest to be addressed by applying an external magnetic field. Consequently, the efficacy of the oxystress will be maximized and the general toxicity minimized. The magnetic properties of the system will allow its detection by MRI and, therefore, it can also be exploited as a theranostic.

Acknowledgements

The authors wish to thank E Caruso for help with Fourier transform infrared spectra.

Financial & competing interests disclosure

This project has been supported by Consorzio Interuniversitario Biotecnologie, Associazione Amici dell'Università and Telecom Working Capital 2011 (Bio and Nanotech) grants. The authors have no other relevant affiliations or financial involvement with any organization or entity with a financial interest in or financial conflict with the subject matter or materials discussed in the manuscript apart from those disclosed.

No writing assistance was utilized in the production of this manuscript.

Ethical conduct of research

The authors state that they have obtained appropriate institutional review board approval or have followed the principles outlined in the Declaration of Helsinki for all human or animal experimental investigations. In addition, for investigations involving human subjects, informed consent has been obtained from the participants involved.

Executive summary

Development of a nanoparticle–enzyme system for cancer therapy

- The method developed for the nanoparticle–enzyme conjugation is reproducible and reliable.

Main characteristics of the nanoparticle–enzyme system

- The system is stable and active for a relatively long time. The use of magnetic nanoparticles allows the system to be directed to the target tissue. The cytotoxicity of the system could be controlled by the addition of appropriate concentrations of the substrate and not strictly dependent on cell type.

Future perspective

- The potentiality of this system should be verified studying tissue distribution, toxicity and clearance after intravenous injection. The efficacy of the oxystress will be maximized addressing Fe_3O_4-3-aminopropyltriethoxysilane–D-amino acid oxidase in the area of interest by applying an external magnetic field. The system's magnetic properties can also be exploited for use as a theranostic.

References

Papers of special note have been highlighted as:
- ▪ of interest
- ▪▪ of considerable interest

1 Cattaneo AG, Gornati R, Sabbioni E *et al.* Nanotechnology and human health: risks and benefits. *J. Appl. Toxicol.* 30, 730–744 (2010).

▪▪ **Comprehensive review balancing the risks and benefits of nanotechnology on human health.**

2 Khanna VK. Targeted delivery of nanomedicines. *ISRN Pharmacol.* 2012, 571394 (2012).

3 Davis ME, Chen ZG, Shin DM. Nanoparticle therapeutics: an emerging treatment modality for cancer. *Nat. Rev. Drug Discov.* 7, 771–782 (2008).

4 De Jong WH, Borm PJ. Drug delivery and nanoparticles: applications and hazards. *Int. J. Nanomedicine* 3(2), 133–49 (2008).

5 Kwon JT, Hwang SK, Jin H *et al.* Body distribution of inhaled fluorescent magnetic nanoparticles in the mice. *J. Occup. Health* 50(1), 1–6 (2008).

6 Lankveld DP, Oomen AG, Krystek P *et al.* The kinetics of the tissue distribution of silver nanoparticles of different sizes. *Biomaterials* 31(32), 8350–8361 (2010).

7 Fang J, Nakamura H, Iyer A. Tumor-targeted induction of oxystress for cancer therapy. *J. Drug Target.* 15, 475–486 (2007).

▪ **Production of PEG-conjugated enzyme for oxystress therapy.**

8 Niculescu-Duvaz I, Springer CJ. Introduction to the background, principles, and state of the art in suicide gene therapy. *Mol. Biotechnol.* 30, 71–88 (2005).

9 Fukumura D, Jain RK. Tumor microenvironment abnormalities: causes, consequences, and strategies to normalize. *J. Cell. Biochem.* 101, 937–949 (2007).

10 Jain RK. Normalization of tumor vasculature: an emerging concept in antiangiogenic therapy. *Science* 307, 58–62 (2005).

11 Nacev A, Kim SH, Rodriguez-Canales J, Tangrea MA, Shapiro B, Emmert-Buck MR. A dynamic magnetic shift method to increase nanoparticle concentration in cancer metastases: a feasibility study using simulations on autopsy specimens. *Int. J. Nanomedicine* 6, 2907–2923 (2011).

12 Jain KK. Advances in the field of nanooncology. *BMC Med.* 8, 83–93 (2010).

13 Barakat IAH, Abbas OA, Ayad S, Hassan AM. Evaluation of radio protective effects of wheat germ oil in male rats. *J. Am. Sci.* 7, 664–673 (2011).

14 Lee Koo YE, Reddy GR, Bhojani M *et al.* Brain cancer diagnosis and therapy with nanoplatforms. *Adv. Drug Deliv. Rev.* 58, 1556–1577 (2006).

15 Paillard F. Cancer gene therapy using oxidative stress. *Hum. Gene Ther.* 9, 159–160 (1998).

▪ **One of the first examples of enzyme oxystress treatment.**

16 Ben-Yoseph O, Ross BD. Oxidation therapy: the use of a reactive oxygen species-generating enzyme system for tumor treatment. *Br. J. Cancer* 70, 1131–1135 (1994).

17 Connors TA. The choice of prodrugs for gene directed enzyme prodrug therapy of cancer. *Gene Ther.* 2, 702–709 (1995).

18 Pollegioni L, Piubelli L, Sacchi S, Pilone MS, Molla G. Physiological functions of D-amino acid oxidases: from yeast to humans. *Cell. Mol. Life Sci*. 64, 1373–1394 (2007).

▪▪ **Comprehensive review of structure–function relationships in D-amino acid oxidase.**

19 Stegman LD, Zheng H, Neal ER *et al.* Induction of cytotoxic oxidative stress by D-alanine in brain tumor cells expressing *Rhodotorula gracilis* D-amino acid oxidase: a cancer gene therapy strategy. *Hum. Gene Ther.* 9, 185–193 (1998).

20 Pollegioni L, Langkau B, Tischer W, Ghisla S, Pilone MS. Kinetic mechanism of D-amino acid oxidases from *Rhodotorula gracilis* and *Trigonopsis variabilis*. *J. Biol. Chem*. 268, 13850–13857 (1993).

21 Rosini E, Pollegioni L, Ghisla S, Orru R, Molla G. Optimization of D-amino acid oxidase for low substrate concentrations – towards a cancer enzyme therapy. *FEBS J.* 276, 4921–4932 (2009).

22 Pankhurst QA, Connolly J, Jones SK, Dobson J. Applications of magnetic nanoparticles in biomedicine. *J. Phys. D. Appl. Phys.* 36, R167–R181 (2003).

23 Arruebo M, Fernández-Pacheco R, Ibarra MR, Santamaría J. Magnetic nanoparticles for drug delivery. *Nano. Today* 2(3), 22–32 (2007).

24 Dobson J. Magnetic nanoparticles for drug delivery. *Drug Dev. Res*. 67, 55–60 (2006).

25 Yoo D, Lee JH, Shin TH, Cheon J. Theranostic magnetic nanoparticles. *Acc. Chem. Res.* 44(10), 863–874 (2012).

26 Harford-Wright E, Lewis KM, Vink R. Towards drug discovery for brain tumors: interaction of kinins and tumors at the blood brain barrier interface. *Recent Pat. CNS Drug Discov*. 6, 31–40 (2011).

27 Rabanel JM, Aoun V, Elkin I, Mokhtar M, Hildgen P. Drug-loaded nanocarriers: passive targeting and crossing of biological barriers. *Curr. Med. Chem.* 19(19), 3070–3102 (2012).

28 Liu Y, Lu W. Recent advances in brain tumor-targeted nano-drug delivery system. *Expert Opin. Drug Deliv.* 9(6), 671–686 (2012).

29 Nair BG, Varghese SH, Nair R, Yoshida Y, Maekawa T, Kumar DS. Nanotechnology platforms; an innovative approach to brain tumor therapy. *Med. Chem.* 7(5), 488–503 (2011)

30 Fantinato S, Pollegioni L, Pilone MS. Engineering, expression and purification of a His-tagged chimeric D-amino acid oxidase from *Rhodotorula gracilis*. *Enz. Microbiol. Technol*. 29, 407–412 (2001).

31 del Campo A, Sen T, Lellouche JP, Bruce IJ. Multifunctional magnetite and silica–magnetite nanoparticles: synthesis, surface activation and applications in life sciences. *J. Magn. Magn. Mater.* 293, 33–40 (2005).

32 Molla G, Porrini D, Job V *et al.* Role of arginine 285 in the active site of *Rhodotorula gracilis*. *J. Biol. Chem.* 275, 24715–24721 (2000).

33 Harris CM, Molla G, Pilone MS, Pollegioni L. Studies on the reaction mechanism in *Rhodotorula gracilis* D-amino acid oxidase. *J. Biol. Chem*. 274, 36233–36240 (1999).

34 Sacchi S, Bernasconi M, Martineau M *et al.* pLG72 modulates intracellular D-serine levels through its interaction with D-amino acid oxidase: effect on schizophrenia susceptibility. *J. Biol. Chem.* 283(32), 22244–22456 (2008).

35 Pollegioni L, Sacchi S. Metabolism of the neuromodulator D-serine. *Cell. Mol. Life Sci*. 67, 2387–2404 (2010).

▪ **Update on D-serine in the brain.**

36 Papis E, Rossi F, Raspanti M *et al.* Engineered cobalt oxide nanoparticles readily enter cells. *Toxicol. Lett.* 189, 253–259 (2009).

▪▪ **Clear example of nanoparticle internalization.**

37 Cañete M, Soriano J, Villanueva A *et al.* The endocytic penetration mechanism of iron oxide magnetic nanoparticles with positively charged cover: a morphological approach. *Int. J. Mol. Med.* 26(4), 533–539 (2010).

38 Verrax J, Beck R, Dejeans N *et al.* Redox-active quinones and ascorbate: an innovative cancer therapy that exploits the vulnerability of cancer cells to oxidative stress. *Anticancer Agents Med. Chem*. 11(2), 213–221 (2011).

39 Manthe RL, Foy SP, Krishnamurthy N, Sharma B, Labhasetwar V. Tumor ablation and nanotechnology. *Mol. Pharm.* 7(6), 1880–1898 (2010).

40 Mohapatra S, Pramanik N, Mukherjee S, Ghosh SK, Pramanik P. A simple synthesis of amine-derivatised superparamegnetic iron oxide nanoparticles for bioapplications. *J. Mater. Sci*. 42, 7566–7574 (2007).

41 Yamaura M, Camilo RL, Sampaio LC, Macêdo MA, Nakamura M, Toma HE. Preparation and characterization of (3-aminopropyl)triethoxysilane-coated magnetite nanoparticles. *J. Magn. Magn. Mat.* 279, 210–217 (2004).

42 Kuan IC, Wu JC, Lee SL, Tsai CW, Chuang CA, Yu CY. Stabilization of D-amino acid oxidase from *Rhodosporidium toruloides* by encapsulation in polyallylamine-mediated biomimetic silica. *Biochem. Eng. J.* 49, 408–413 (2010).

43 Chien LJ, Lee CK. Biosilicification of dual-fusion enzyme immobilized on magnetic nanoparticle. *Biotechnol. Bioeng.* 100, 223 (2008).

44 Hsieh HC, Kuan IC, Lee SL, Tien GY, Wang YJ, Yu CY. Stabilization of D-amino acid oxidase from *Rhodosporidium toruloides* by immobilization onto magnetic nanoparticles. *Biotechnol. Lett.* 31, 557–563 (2009).

45 Naqvi S, Samim M, Abdin M *et al.* Concentration-dependent toxicity of iron oxide nanoparticles mediated by increased oxidative stress. *Int. J. Nanomedicine* 5, 983–989 (2010)

46 Prijic S, Scancar J, Romih R *et al.* Increased cellular uptake of biocompatible superparamagnetic iron oxide nanoparticles into malignant cells by an external magnetic field. *J. Membr. Biol.* 236, 167–179 (2010).

47 Xin-li L, Shu-Hua Z, Long Z, Gui-Qin H, Zhi-Wei S, Wen-Sheng Y. Dose dependent cytotoxicity and oxidative stress induced by 'naked' Fe_3O_4 naoparticles in human hepatocyte. *Chem. Res. Chinese Universities* 28(1), 114–118 (2012).

48 Gazeau F, Wilhelm C. Magnetic labeling, imaging and manipulation of endothelial progenitor cells using iron oxide nanoparticles. *Future Med. Chem.* 2, 397–408 (2010).

49 Thorek DL, Tsourkas A. Size, charge and concentration dependent uptake of iron oxide particles by nonphagocytic cells. *Biomaterials* 29(26), 3583–3590 (2008).

50 Divakaran SA, Sreekanth KM, Rao KV, Nair CKK. D-aminoacid oxidase–Fe_2O_3 nanoparticle complex mediated antitumor activity in swiss albino mice. *J. Cancer Ther.* 2, 666–674 (2011).